Supplementary Information

New insights on ruthenium(II) metallodendrimers as anticancer drugs nanocarriers: from synthesis to preclinic behaviour

Dina Maciel,[a] Nádia Nunes,[a] Francisco Santos,[a] Yu Fan,[b] Gaoming Li,[b] Mingwu Shen,[b] Helena Tomás,[a] Xiangyang Shi,[ab] and João Rodrigues [*a]

[a]CQM - Centro de Química da Madeira, MMRG, Universidade da Madeira, Campus Universitário da Penteada, 9020-105 Funchal, Portugal.

[b]College of Chemistry, Chemical Engineering and Biotechnology, Donghua University, Shanghai, 201620, China.

*E-mail:joaor@uma.pt/joaoc@staff.uma.pt

Content

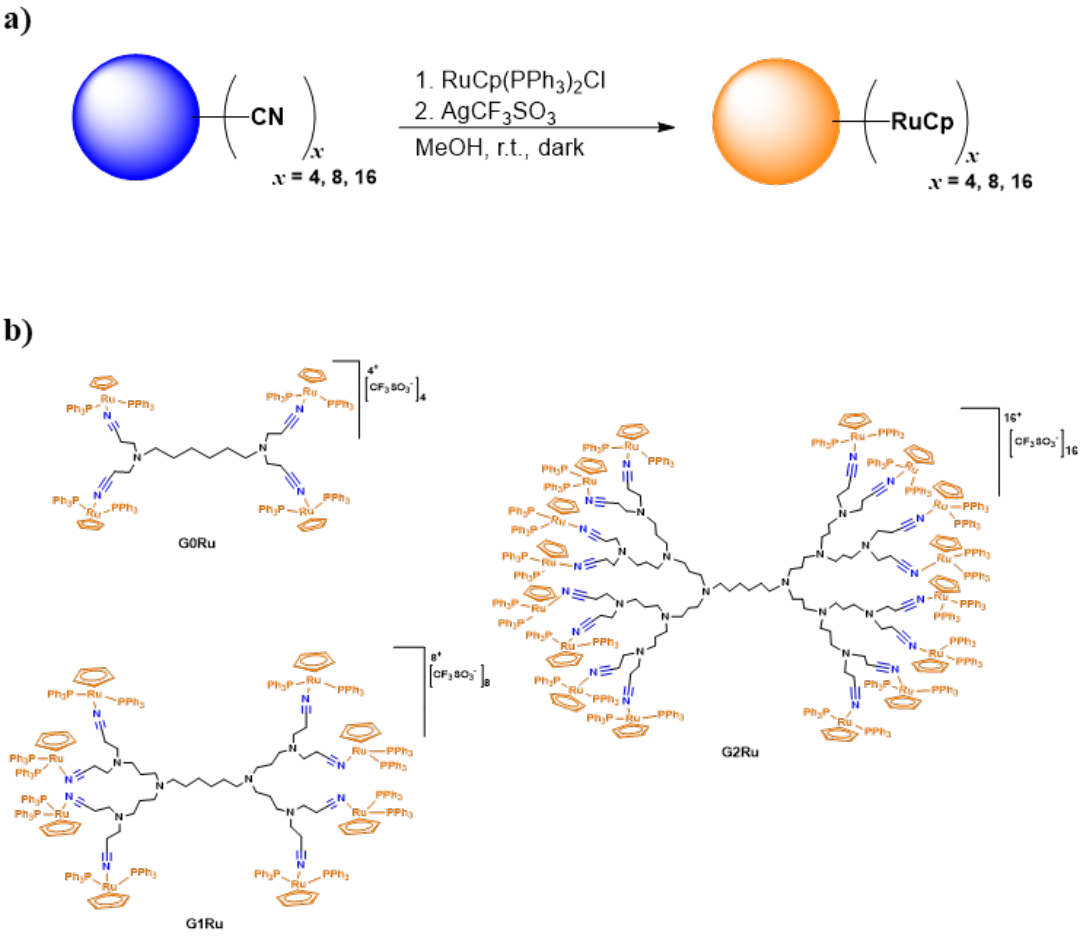

Fig. S1 a) Synthesis of the ruthenium metallodendrimers and b) Structural representation of the prepared G0Ru – G2Ru metallodendrimers.

a)

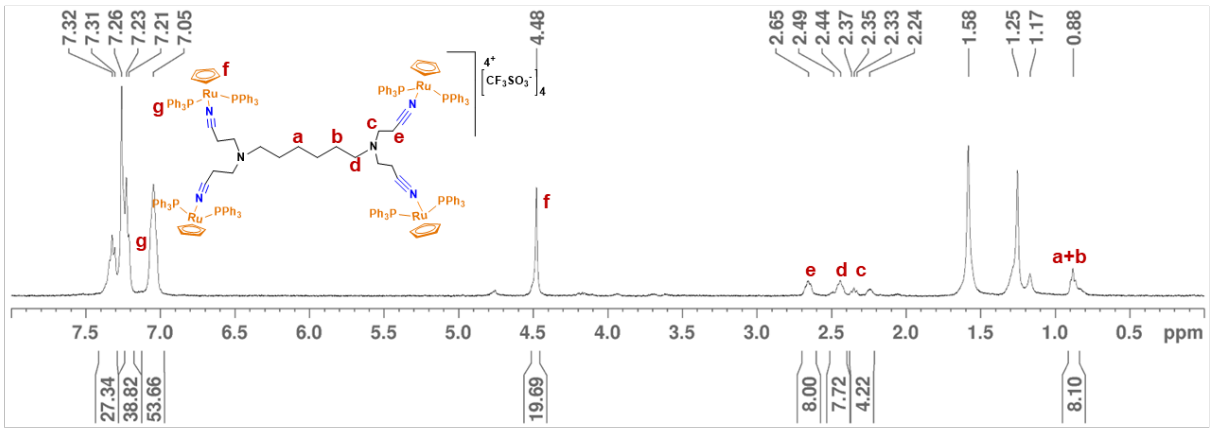

b)

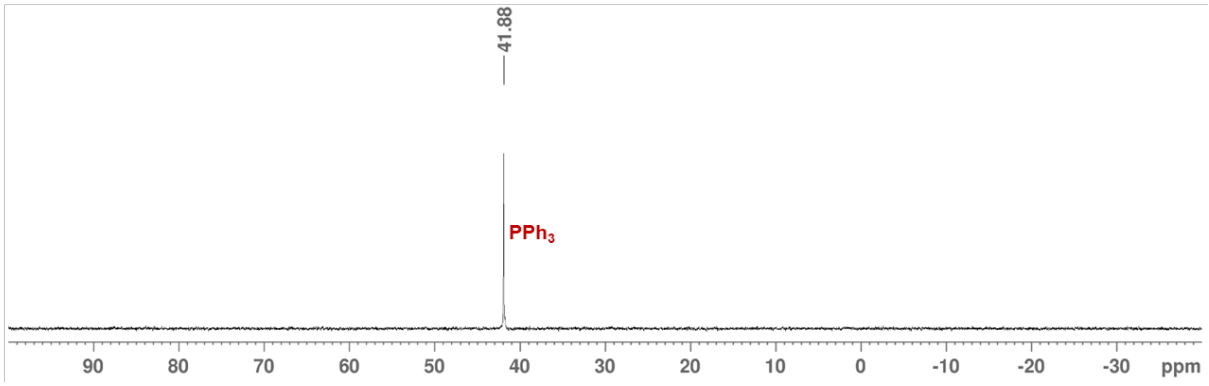

Fig. S2 a) ^{1}H-NMR and b) ^{31}P-NMR spectra of the G0Ru metallodendrimer performed in $CDCl_3$.

a)

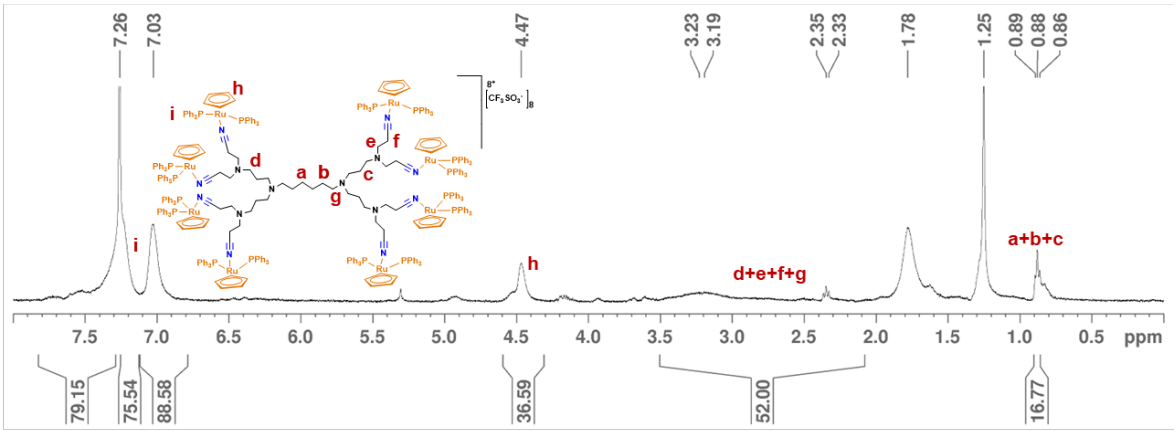

b)

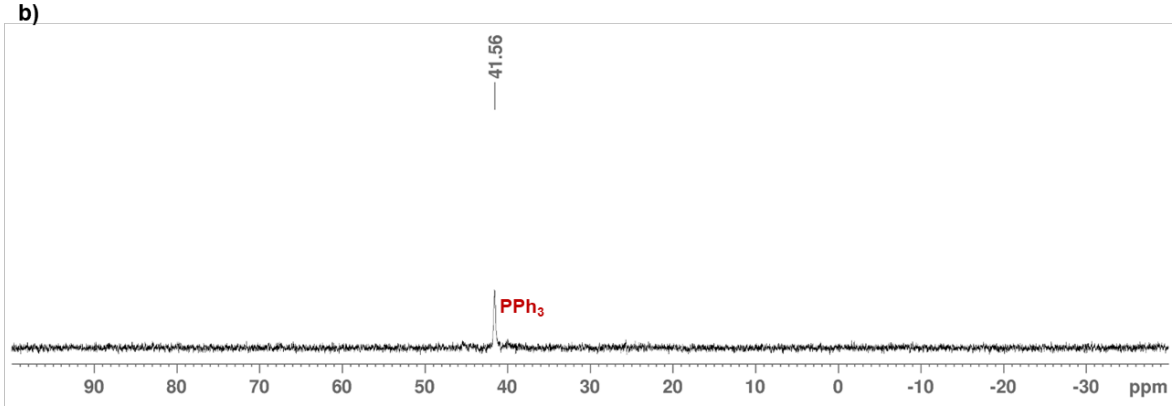

Fig. S3 a) ^{1}H-NMR and b) ^{31}P-NMR spectra of the G1Ru metallodendrimer performed in $CDCl_3$.

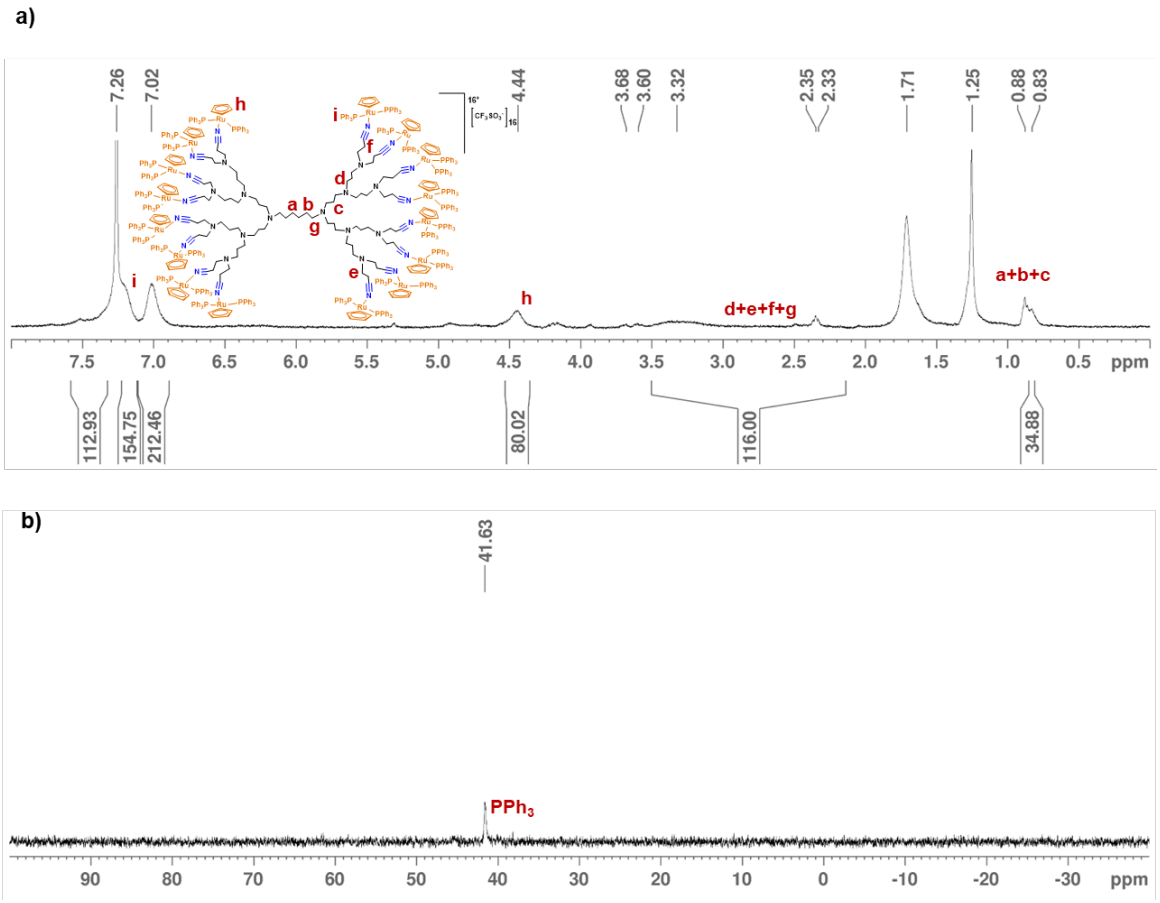

Fig. S4 a) ^{1}H-NMR and b) ^{31}P-NMR spectra of the G2Ru metallodendrimer performed in $CDCl_3$.

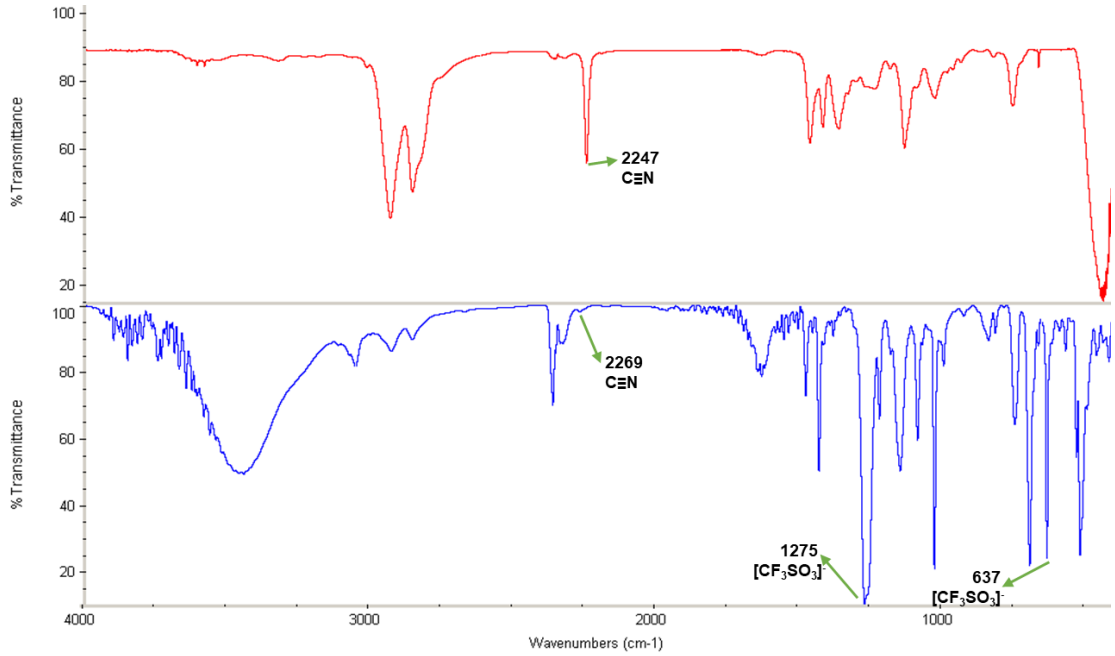

Fig. S5 FT-IR spectra of the G0CN dendrimer (above) and G0Ru metallodendrimer (below). G0CN was performed using NaCl cells and G0Ru in KBr pellets.

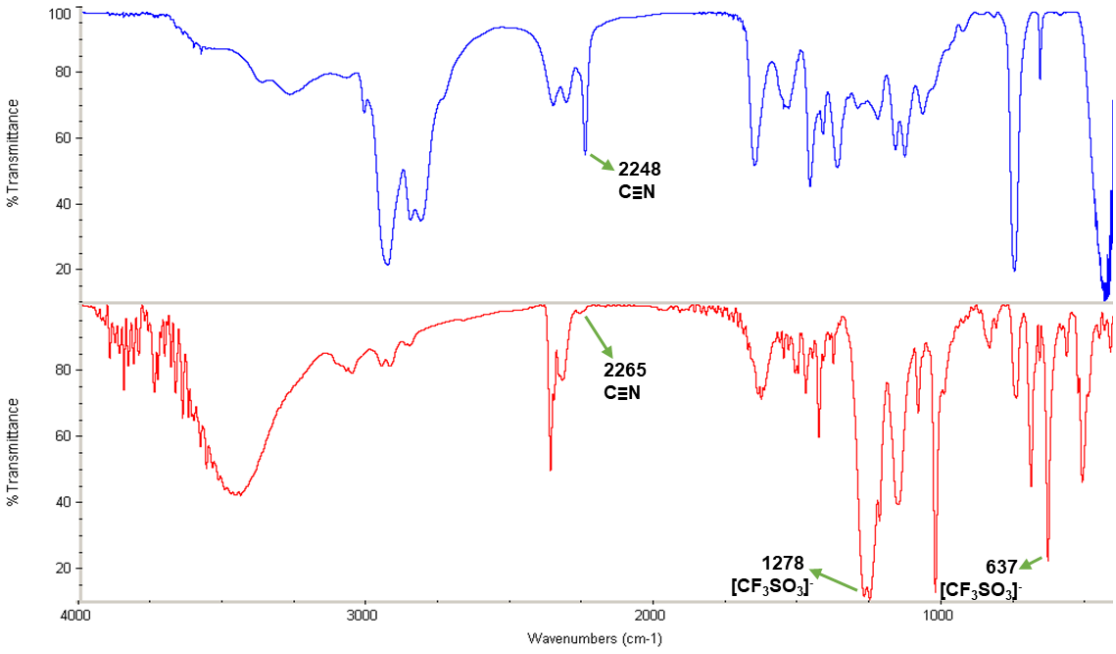

Fig. S6 FT-IR spectra of the G1CN dendrimer (above) and G1Ru metallodendrimer (below). G1CN was performed in the NaCl cells and G1Ru in KBr pellets.

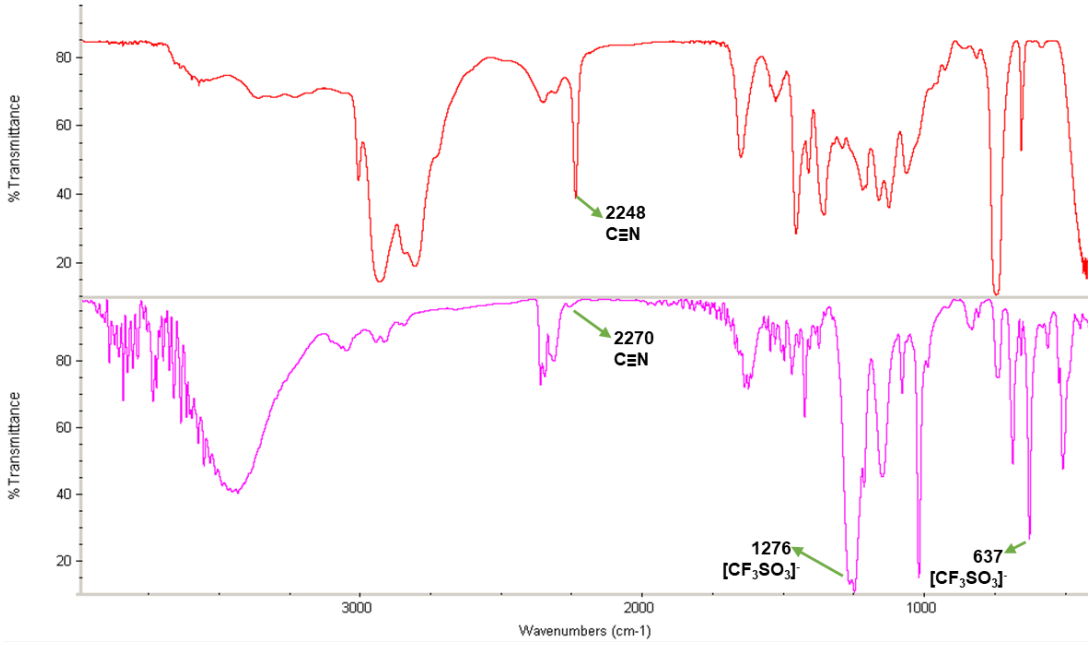

Fig. S7 FT-IR spectra of the G2CN dendrimer (above) and G2Ru metallodendrimer (below). G2CN was performed in the NaCl cells and G2Ru in KBr pellets.

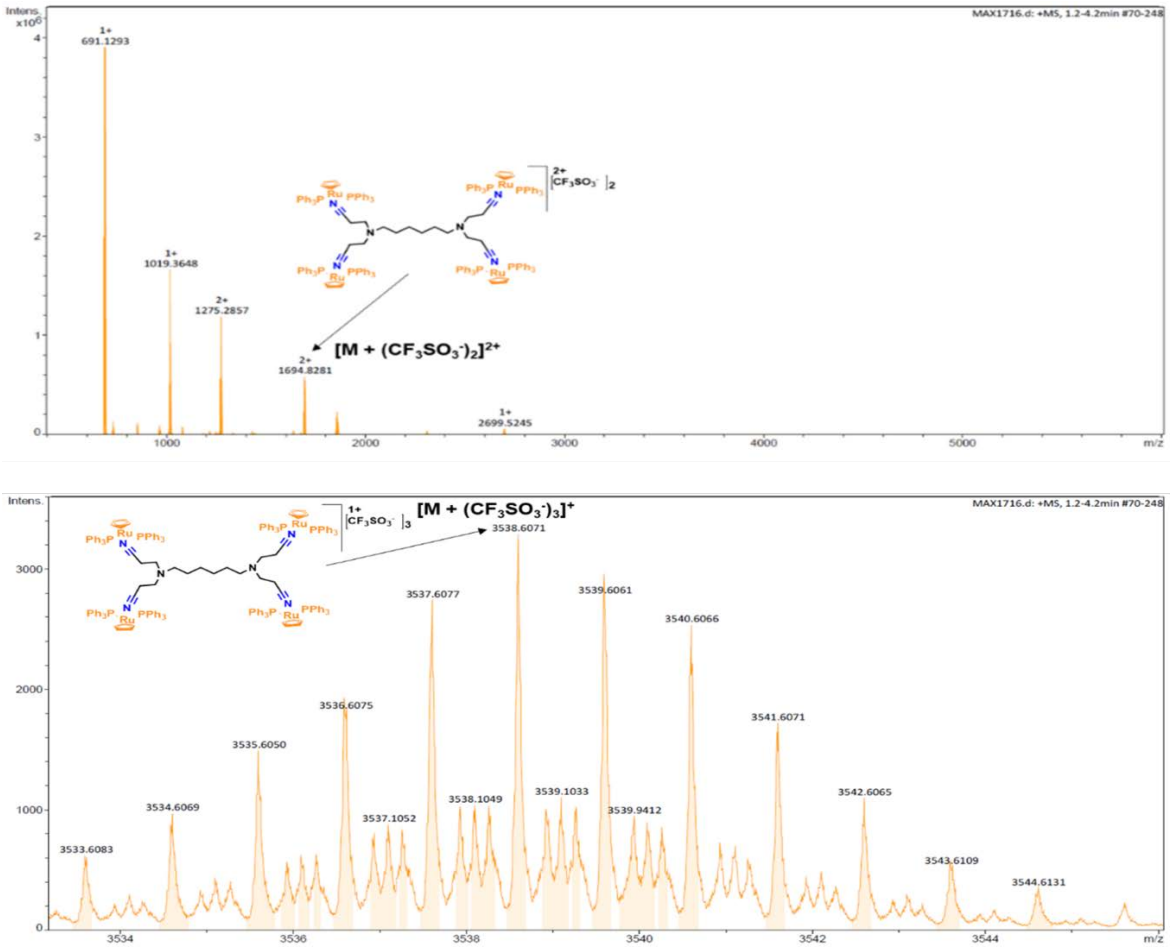

Fig. S8 Mass spectra of G0Ru metallodendrimer.

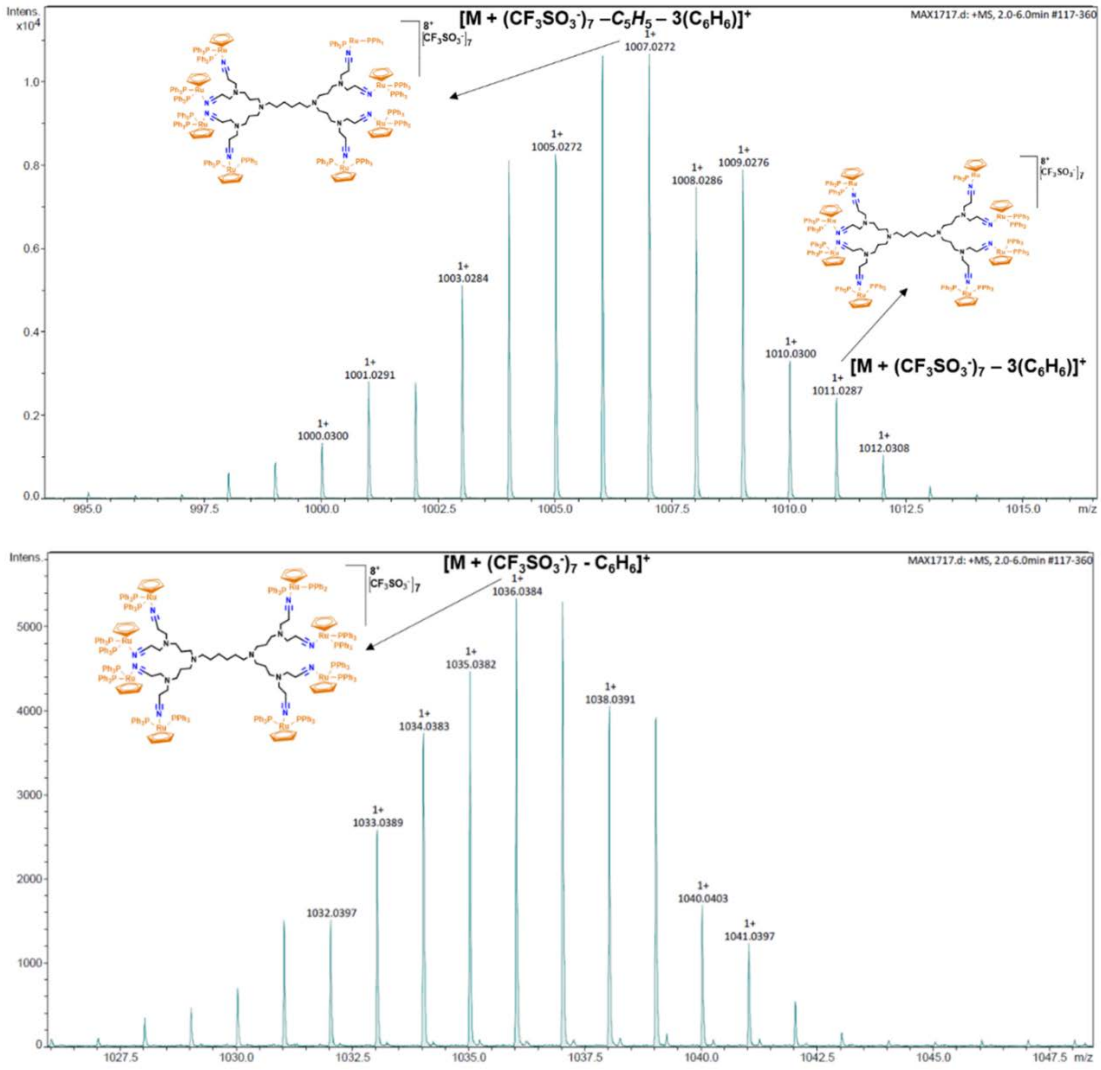

Fig. S9 Mass spectra of G1Ru metallodendrimer.

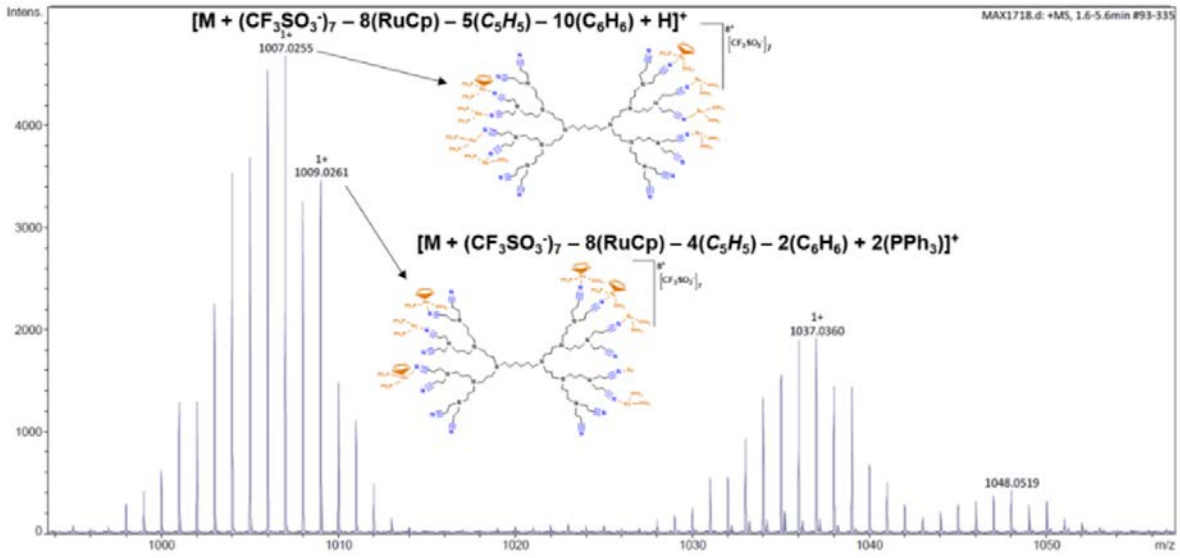

Fig. S10 Mass spectrum of G2Ru metallodendrimer.

Table S1. Size, zeta potential, and polydispersity index measurements of the ruthenium metallodendrimers. Data are represented as mean ± SD of five independent experiments.

	Size (nm)	Zeta Potential (mV)	Polydispersity index
G0Ru	115.5 ± 4.6	29.9 ± 2.0	0.177 ± 0.013
G1Ru	60.2 ± 4.5	40.7 ± 0.6	0.267 ± 0.049
G2Ru	208.7 ± 7.3	41.7 ± 1.6	0.247 ± 0.007

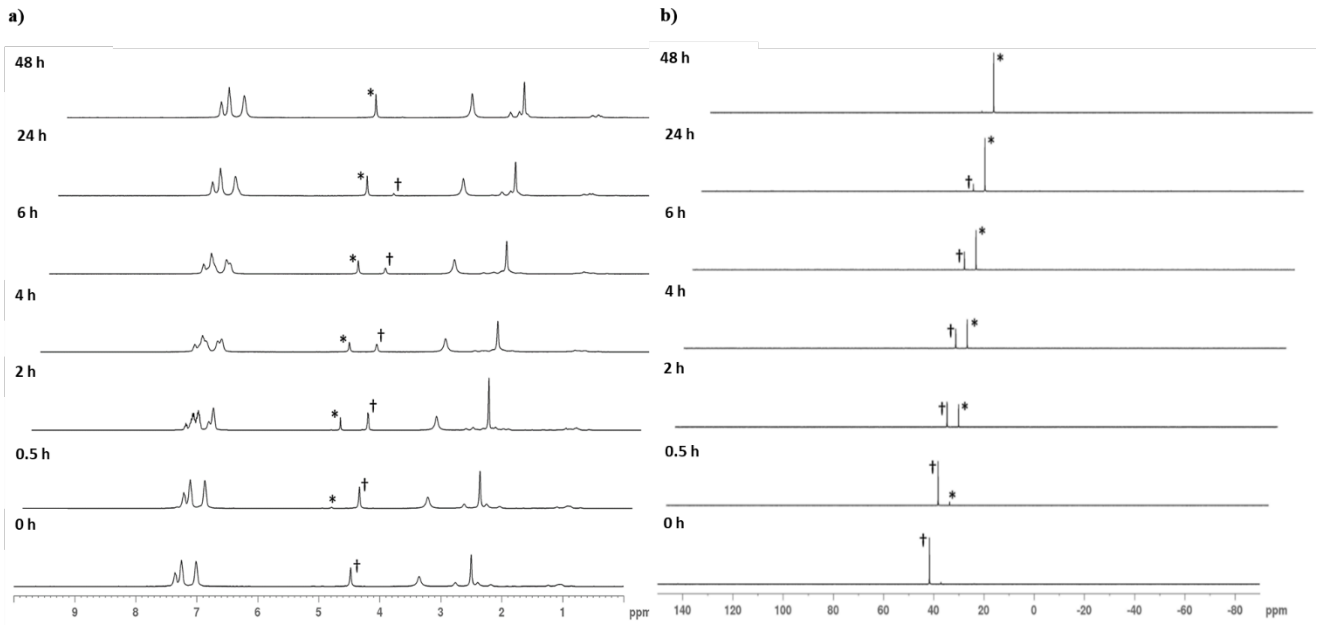

Fig. S11 ^{1}H-NMR and ^{31}P-NMR spectra of G0Ru metallodendrimer were performed in DMSO-d_6. Stability studies were carried out at a probe temperature of 25°C. a) ^{1}H-NMR: † = proton signal from the cyclopentadienyl of the metallodendrimer, * = proton signal from the cyclopentadienyl of the RuCp complex. b) ^{31}P-NMR: † = phosphorous signal from the phosphines of the metallodendrimer, * = phosphorous signal from the phosphines of the RuCp complex.

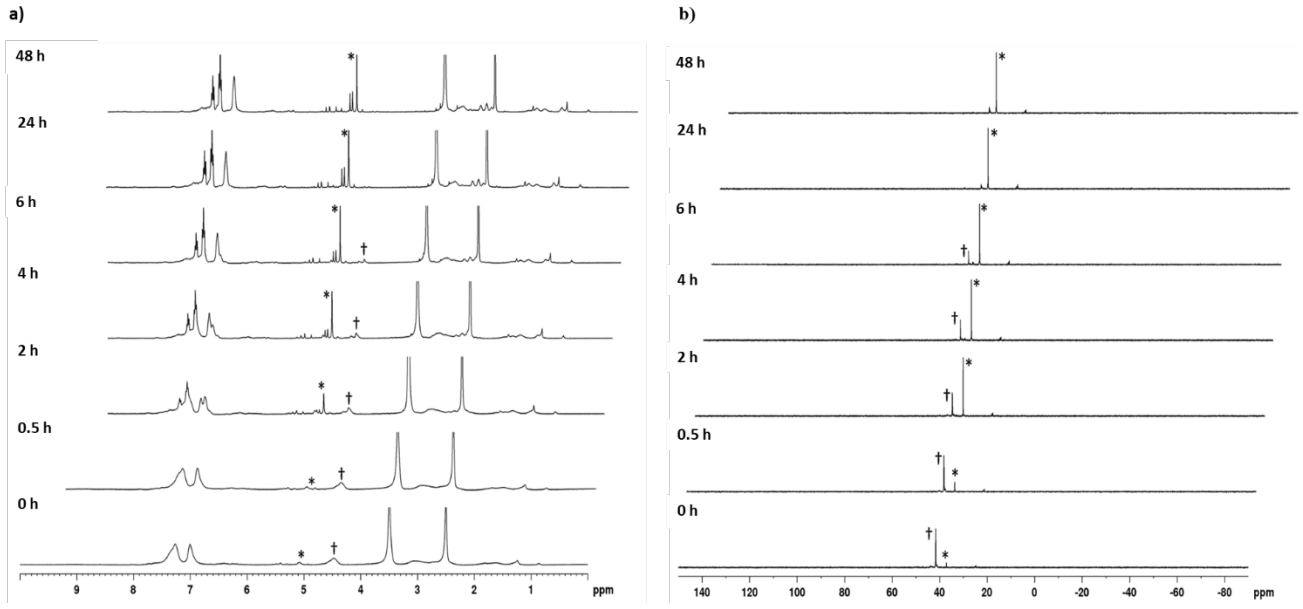

Fig. S12 ^{1}H-NMR and ^{31}P-NMR spectra of G1Ru metallodendrimer were performed in DMSO-d_6. Stability studies were carried out at a probe temperature of 25°C. a) ^{1}H-NMR: † = proton signal from the cyclopentadienyl of the metallodendrimer, * = proton signal from the cyclopentadienyl of the RuCp complex. b) ^{31}P-NMR: † = phosphorous signal from the phosphines of the metallodendrimer, * = phosphorous signal from the phosphines of the RuCp complex.

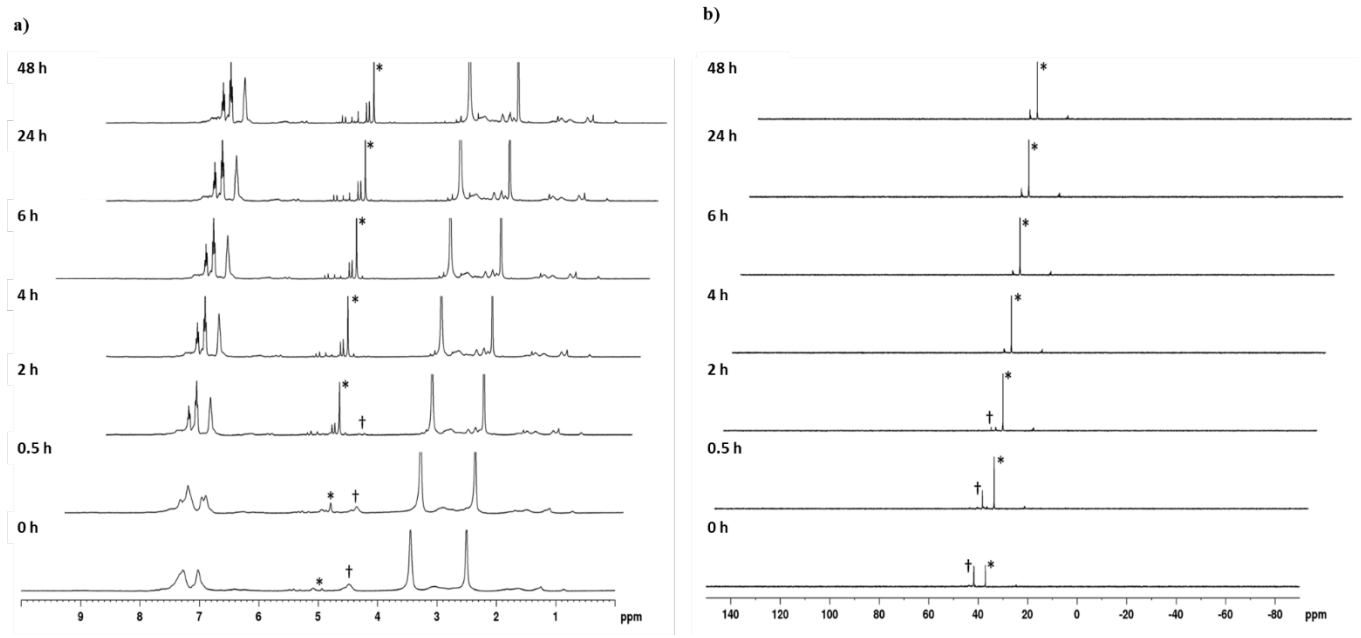

Fig. S13 ^{1}H-NMR and ^{31}P-NMR spectra of G1Ru metallodendrimer were performed in DMSO-d_6. Stability studies were carried out at a probe temperature of 37°C. a) ^{1}H-NMR: † = proton signal from the cyclopentadienyl of the metallodendrimer, * = proton signal from the cyclopentadienyl of the RuCp complex. b) ^{31}P-NMR: † = phosphorous signal from the phosphines of the metallodendrimer, * = phosphorous signal from the phosphines of the RuCp complex.

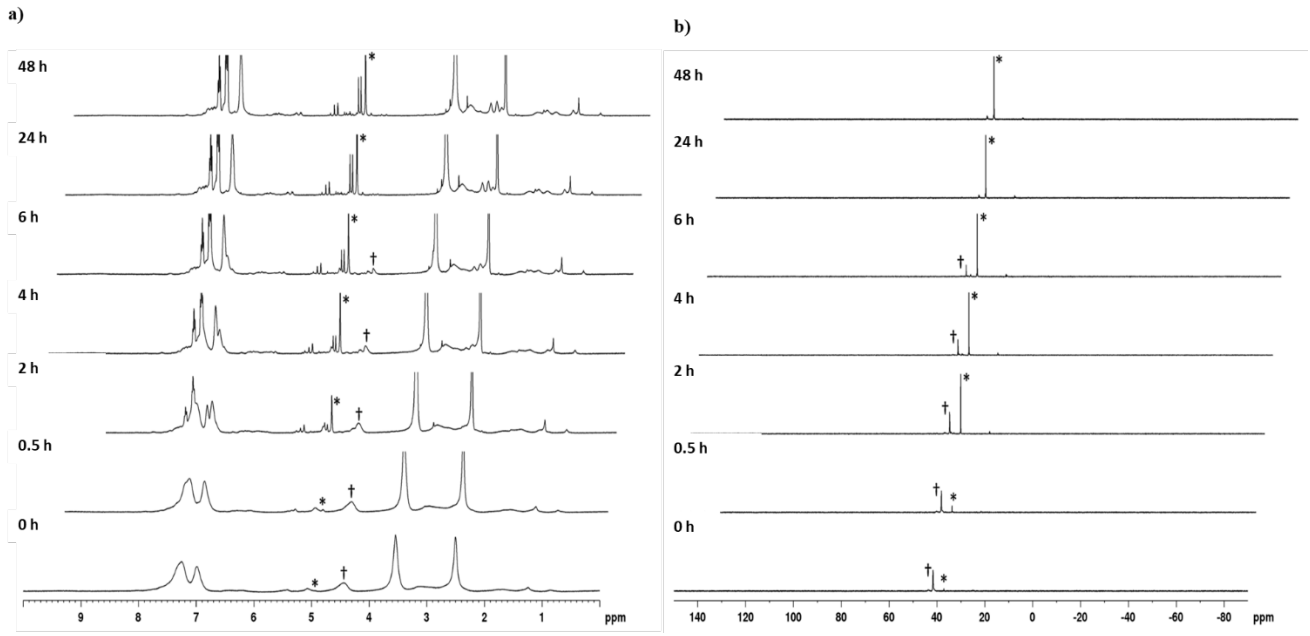

Fig. S14 ^{1}H-NMR and ^{31}P-NMR spectra of G2Ru metallodendrimer were performed in DMSO-d_6. Stability studies were carried out at a probe temperature of 25°C. a) ^{1}H-NMR: † = proton signal from the cyclopentadienyl of the metallodendrimer, * = proton signal from the cyclopentadienyl of the RuCp complex. b) ^{31}P-NMR: † = phosphorous signal from the phosphines of the metallodendrimer, * = phosphorous signal from the phosphines of the RuCp complex.

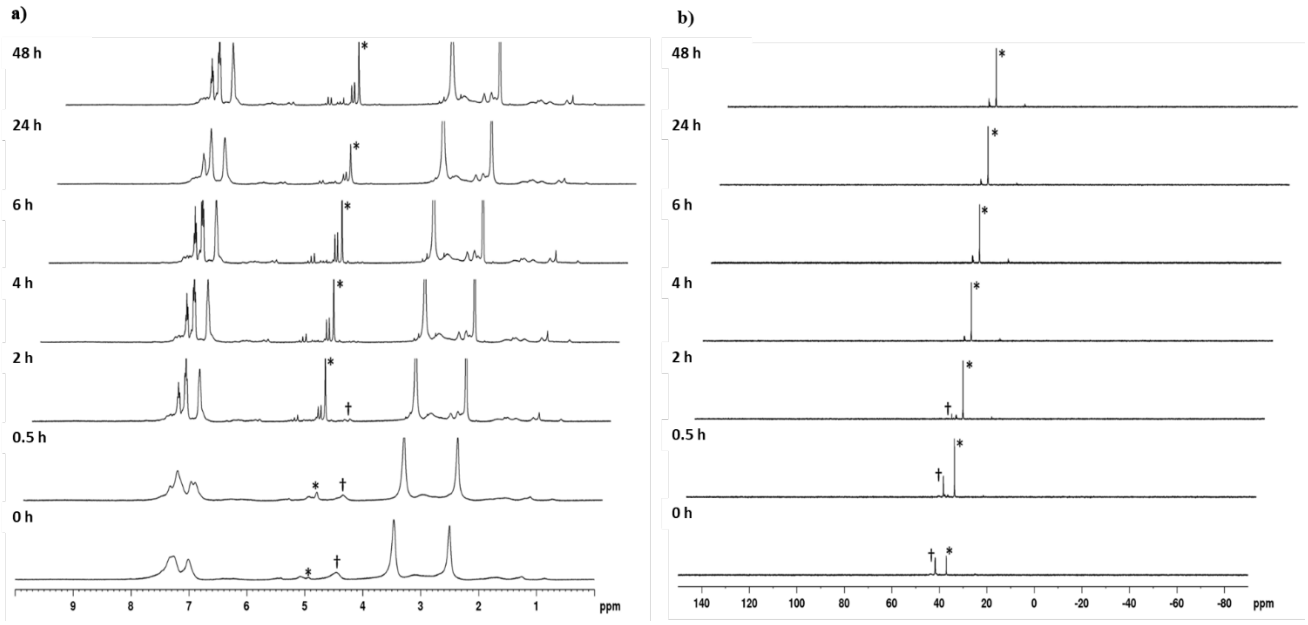

Fig. S15 ^{1}H-NMR and ^{31}P-NMR spectra of G2Ru metallodendrimer were performed in DMSO-d_6. Stability studies were carried out at a probe temperature of 37°C. a) ^{1}H-NMR: † = proton signal from the cyclopentadienyl of the metallodendrimer, * = proton signal from the cyclopentadienyl of the RuCp complex. b) ^{31}P-NMR: † = phosphorous signal from the phosphines of the metallodendrimer, * = phosphorous signal from the phosphines of the RuCp complex.

Table S2. Cytotoxic concentration of ruthenium in the metallodendrimers against A2780, A2780cisR, CAL-72, U-87MG, Caco-2, and MCF-7 cancer cell lines and hMSCs as a non-cancer cell line.

Compound	M[a)]	[Ru, µM]						
		A2780	A2780cisR	CAL-72	U-87MG	Caco-2	MCF-7	hMSC
RuCp	1	0.5	0.7	0.6	0.5	0.6	0.4	3.9
G0Ru	4	1.2	1.0	1.6	1.4	1.5	1.3	3.3
G1Ru	8	1.2	1.8	2.4	1.4	2.1	1.8	6.6
G2Ru	16	1.1	1.1	1.8	1.3	1.3	1.4	6.4

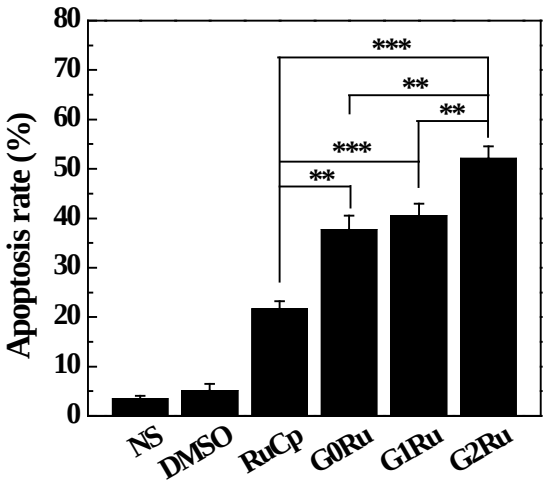

Fig. S16 Apoptosis rates in different groups by quantification of the TUNEL-positive tumour cells in tumour sections.

Table S3. The *in vitro* IC_{50} values of the metallodendrimers using MCF-7 and hMSCs and the *in vivo* concentration of the metallodendrimers, and the corresponding ruthenium concentration.

		in vitro		***in vivo***	
Compound	**Metal centres**	**MCF-7 (IC_{50}, μM)**	**hMSC (IC_{50}, μM)**	**[metallodendrimer, μM]**	**[Ru, μM]**
RuCp	1	0.37 ± 0.03	3.89 ± 0.3	650	650
G0Ru	4	0.33 ± 0.02	0.83 ± 0.07	162.5	650
G1Ru	8	0.23 ± 0.05	0.83 ± 0.04	162.5	1310
G2Ru	16	0.09 ± 0.01	0.39 ± 0.3	162.5	2620